Environmental Science Nano

Real-time assessment of the impacts of polystyrene and silver nanoparticles on hatching process and early-stage development of *Artemia* using a microfluidic platform

Journal:	*Environmental Science: Nano*
Manuscript ID	EN-ART-02-2024-000116.R1
Article Type:	Paper

Real-time assessment of the impacts of polystyrene and silver nanoparticles on hatching process and early-stage development of *Artemia* using a microfluidic platform

Preyojon Dey [a], Terence M. Bradley [b] and Alicia Boymelgreen*[a]

a. Department of Mechanical and Materials Engineering, Florida International University, 10555 W Flagler St, Miami, FL, 33174, USA.

b. Department of Fisheries, Animal and Veterinary Science, University of Rhode Island, Kingston, RI 02881, USA.

* Corresponding author, E-mail: aboymelg@fiu.edu

Abstract

Development of real-time in-situ monitoring techniques is crucial for a mechanistic understanding of the impacts of pollution on the marine environment. Here, we investigate how different nanopollutants impact the vulnerable hatching process and early-stage development of marine organisms, by observing real-time oxygen consumption and morphological changes using a microfluidic platform. We compare the effects of polystyrene (PS) and silver (Ag) nanoparticles (NPs) at environmentally relevant NP doses from 0-1 mg/L on the hatching process and nauplius stage of *Artemia*. The four stages of *Artemia* hatching - hydration, differentiation, emergence, and hatching - are distinguished by both metabolism and morphology. NP exposure altered the hydration duration at the lowest dose, prolonging differentiation, and slowing emergence from the cysts resulting in a shortened hatching period. NPs also increased oxygen demand in every hatching stage except differentiation. Overall hatchability rose with NP concentration, while survivability showed an inverse trend. This might be attributed to increased NP aggregation in saltwater at higher concentrations which decreases bioavailability during hatching but not post-hatch consumption. Overall, Ag NPs had a greater impact on hatching and mortality than PS NPs. Both NPs significantly affected swimming speed, however, while PS NPs decreased speed, Ag NPs increased it.

Keywords: Nanoplastic, Ag, Toxicity, Oxygen consumption, Metabolic rate, Bioaccumulation

Environmental significance

Aquatic nanopollution from terrestrial sources including plastics and heavy metals is a growing environmental concern. These pollutants threaten aquatic ecosystems, especially during critical reproductive and early life stages, potentially affecting their distribution. While traditional end-point assessments offer broad insights into these impacts, the need for a mechanistic understanding is paramount. Real-time monitoring on a microfluidic platform can be a key. Using such a platform we investigated how plastic and metal nanoparticles affected *Artemia*'s stage duration and respiration, causing hatching inhibition, altered swimming, and mortality. This study not only offers detailed insights on the consequences of nanopollution for aquatic species but also demonstrates the potential of this setup for evaluating the impacts of other aquatic pollutants, thereby promoting environmental protection measures.

1. Introduction

Rivers, runoff, and direct discharges transport contaminants from human activities into oceans, with plastic being the dominant marine pollutant, making up 80-85% of marine litter (1–3). Annually, nearly 8 million tons of plastic enter the ocean(2), mostly from land-based sources (4), breaking down into micro and nanoparticles (MNPs) through various processes (5,6). Macro-sized plastics or macroplastics (5-100 mm) fracture over time in marine environments, forming secondary micro (<5 mm) and nanoplastics (<100 nm) (7). It is estimated that the size distribution of these is with 70–80% secondary microplastics (7–9), and only 15-30% are primary microplastics (7,9). Information on the quantity of marine nanoplastics content is still scarce in the literature. Meanwhile, nanotechnology has boosted metallic nanoparticle (NP) production, posing new marine pollution concerns (10,11). This study used two types of model nanoparticles: polystyrene (PS) and silver (Ag). PS, accounting for 23 million tons of annual global plastic

production (12), contributes significantly to marine debris (13–15) . Ag NPs are widely used in medical applications (16), biosensors (17), electronics (18), textiles (19), and more, posing water contamination risks due to their high toxicity [35,]

While a large number of studies have focused on microparticles (MPs) (21–24), NPs may pose greater harm (25) due to size-related properties, enabling wider dispersal (26,27), mistaken ingestion by marine life (28,29), and prompt toxin release (30,31). Vulnerable reproductive and early life stages of marine species are at risk (32,33), potentially impacting ecosystems (34,35). The diversity of nanopollutants may have modified effects (36,37) and thus necessitates comparative analyses of the effects at relevant concentrations. It is important to note that MNPs behave differently in freshwater and saltwater, with saltwater promoting agglomeration (38), potentially impacting MNPs' bioavailability and aquatic organisms differently from freshwater environments (39–41). Previously, PS and Ag NPs have been studied on *Brachionus plicatilisi* (42), and *Oryzias latipes* (43), revealing that both types of NPs are toxic. Here, a zooplankton species, commonly used as live feed in marine finfish larviculture due to its small size and rich nutrient content (44,45), *Artemia franciscana*, was used to examine the toxic effects of these two NPs on both the hatching process and nauplius stage. *Artemia* are found in inland saltwater lakes and coastal lagoons characterized by a hypersaline environment (46,47), which serves as their sole means of defense against predators (47,48). Nevertheless, they possess the ability to adapt to a broad spectrum of salinity (49), making them suitable candidates for investigating the comparative toxicity of nanoparticles in water with salinity comparable to the oceanic environment. Previously, this species has been widely used as an aquatic model animal in ecological, ecotoxicological, genetic, biochemical, and physiological studies [33–35]. The ISO/TS 20787:2017 standard proposes that the hatching rate of *Artemia* can be used as the outcome for acute nanomaterial environmental

toxicity tests (50). Previous comparative studies on the impacts of different NPs on *Artemia* focused primarily on the larval or adult stages (51–57) with few studies evaluating the impacts of different NPs on hatching rate (HR) (58–61). These studies demonstrated a significant decrease in hatching rate in the presence of NPs, using conventional endpoint toxicity assessment along with survival and mobility.

The current work employs a microfluidic platform with an integrated optical oxygen sensor to provide real-time information on the hatching process and early-stage development to understand the mechanisms that inhibit hatching and cause mortality and altered swimming. This platform allowed real-time tracking of *Artemia* respiration during hatching, correlating physical changes observed under a microscope with sensor data to assess their impact on hatching (62). Automatic handling and counting on the microfluidic platform enhanced hatchability estimation accuracy (62). Prior studies have employed micro and milli-fluidic platforms for live animals (63–65), including zebrafish (66–68), and various respirometry techniques have measured oxygen consumption in marine species exposed to contaminants (69–71). This microfluidic system, compact and capable of temperature control, minimizes sensor noise (72–77) and provides consistent hatching conditions. In a previous study by our group (62), a similar setup was used to evaluate optimal hatching conditions for *Artemia*, where it was observed hatching stage could be identified through metabolic rates and morphology and both the temperature and salinity affected the duration of hatching stages, metabolic rates, and hatchability. It is anticipated that the present approach could be employed to shed light on the effects of different environmental conditions and marine nano-pollutants on the hatching and early development of a variety of other marine species.

2. Experimental

50 nm red fluorescent PS NPs in a 1% solids (w/v) aqueous suspension (Fluoro-Max, Cat. No. R50) and 40 nm citrate-capped Ag NPs in a 0.02 mg/ml sodium citrate-stabilized aqueous buffer (Cat. No. J67090.AE) were purchased from Thermo Scientific Chemicals and used in this study without any modification. The morphology, size and aggregation behavior of the NPs were evaluated using scanning electron microscopy (SEM), dynamic light scattering (DLS) and photographs, respectively, as described in Text S1, Supporting Information (SI). PS NPs were spherical, and Ag NPs were irregularly shaped [Figure S1(A&B), SI]. PS and Ag NPs had Z-average sizes of 50.43 ± 0.24 nm and 45.83 ± 0.13 nm, polydispersity index (PDI) of 0.02 ± 0.01 and 0.23 ± 0.00, and Zeta potential of -23.8 ± 0.96 mV and -34.07 ± 1.86 mV [mean ± standard deviation (SD)], respectively.

The *Artemia* cysts utilized in this study are from the *Artemia franciscana* species and were procured from Brine Shrimp Direct. These as-received cysts were mixed at a concentration of 5 g cysts/L with artificial saltwater (ASW) (control) or ASW containing NPs of varying concentrations without any prior treatment. These cysts were then allowed to hatch for 24 hours using a microfluidic platform under a continuous LED light (1W, Amscope) at 25°C and 25 ppt salinity. In this study, four different NP concentrations were used: 0.01, 0.1, 0.5, and 1 mg/L. Marine pollutants, including plastics in oceans, vary by location (78,79), with some regions reporting concentrations as high as 1.26 mg/L (80). Hence, these tested NP concentrations cover a wide range of environmentally relevant doses. ASW was made with Fluval Marine Salt mixed with deionized water according to specified concentration (see SI). The platform's design, fabrication, and operation were detailed in our prior work (62) and briefly discussed in Text S2, SI and presented in Figure S2, SI.

At each NP concentration, hatching experiments were performed in triplicate. The test conditions are described in detail in Text S2, SI. Furthermore, in this study, *Artemia* cysts were hatched not only in saltwater with the initial types of NPs (PS: 50 nm and Ag: 40 nm), but also in DIW with various sizes of PS (50 nm, 2 μm, 10 μm) and Ag (40 and 100 nm) NPs and MPs. This was done to avoid salt crystal formation from ASW evaporation obscuring cyst morphology, simulate geometric interactions with nanoparticle aggregates and solely for the purpose of imaging. This is explained further in Text S2, SI.

The morphology of the as-received cysts, cysts hatched under distinct NP conditions (either in ASW or DIW) and the distribution of NPs on the surface of those cysts are evaluated by SEM and energy dispersive X-ray spectroscopy (EDS), as described in Text S2, SI, and illustrated in Figure S3 and S4, SI. NP conditions, unless otherwise stated in this manuscript, refer to the combination of NP types and NP concentrations. As-received cysts displayed a cup-shaped structure with porous inner walls (160-900 nm pores, Figure S3, SI).

During hatching, morphological alterations in cysts from optical photomicrographs and depletion in dissolved oxygen concentration (DDOC) in the hatching media (ASW or ASW with NPs) (from DDOC vs. hatching time, as illustrated in Figure S5, SI) were utilized to determine different hatching stage durations (details provided in Text S3, SI). The overall rate of oxygen consumption (oROC) was determined to assess the overall impact on oxygen consumption over the 24-hour hatching experiment, by normalizing with the weight of the initial dry cysts used for hatching. Meanwhile, the average rate of oxygen consumption (aROC) was calculated separately for the pre-hatching stages ($aROC_{1\text{-}3}$) and the post-hatching stage ($aROC_4$) to compare the effects of NPs at each individual hatching stage. Hatching rate (HR) and fraction of live *Artemia* (FLA) were also calculated. The calculation methods for all these parameters are described in Text S3 and Text S5,

SI. Mortality rate and swimming speed of newly hatched *Artemia* were also evaluated as conventional endpoint toxicity tests (81,82) and the calculation method is described in detail in Text S4, SI. Briefly, the mortality rate was calculated based on the rate of nonmotile nauplii after 15 sec of manual agitation. This method was utilized in several prior studies to calculate mortality rate (60,81), although in some studies it was also regarded as the immobilization rate (54,55). Moreover, NP uptake by the *Artemia* nauplii was studied using bright field images (Axioscope 5, Zeiss) (Ag NP-exposed), fluorescence images (Nikon eclipse Ti2-E) (PS NP-exposed), and ImageJ for intensity measurement. For this, photographs were captured of live *Artemia* that were collected from the hatching chip after 24 hours of exposure to NPs, placed on glass slides, which were later immobilized because of evaporation of water layer and insufficient water for swimming.

The statistical analyses were performed by one-way analysis of variance (ANOVA), followed by Tukey post-hoc. Additionally, multivariate analyses were also performed for assessing correlations between different studied factors. If $p<0.05$, the results were considered significant. The details are provided in Text S6, SI.

3. Results and Discussion

3.1 Aggregation behavior of PS and Ag nanoparticles in saltwater

High ionic strength reduces the thickness of the electric double layer (EDL), and decreases electrostatic repulsion, leading NPs in saltwater to interact, agglomerate, and settle (83,84), a phenomenon exacerbated by higher temperature (25 ^{0}C) (85). This agglomeration significantly affects NPs' uptake due to changes in their effective radius (86,87). Figure S1 (C&D), SI illustrate this behavior, depicting the hydrodynamic size (Z-average) and polydispersity index (PDI) of different concentrations of PS and Ag NP suspensions in ASW after 1 and 24 hours. Remarkably,

PS NPs aggregate more than Ag NPs, forming larger aggregates even within just one hour (Figure S1(C), SI), and exhibiting higher PDIs than Ag NP suspensions [Figure S1(D), SI], indicating broader size distributions. After 24 hours, both NP suspensions show increased Z-average sizes with concentration, but PS NP suspensions consistently maintain larger aggregates than Ag NP suspensions (24.73 ± 9.75 vs. 2.56 ± 0.56 μm at 1 mg/L concentration). This disparity is also evident in images of the NP suspensions in ASW after 24 hours [Figure S1(E)], with PS NPs showing more substantial sedimentation and larger aggregates. Differences in aggregation behavior can be attributed to the presence of a citrate capping agent in Ag NPs (39,88,89) and variations in particle morphology (90), with PS particles being spherical and Ag particles irregular, influencing aggregation kinetics and PDI trends.

3.2 Hatching stages of *Artemia,* real-time monitoring and interaction with nanoparticles during hatching

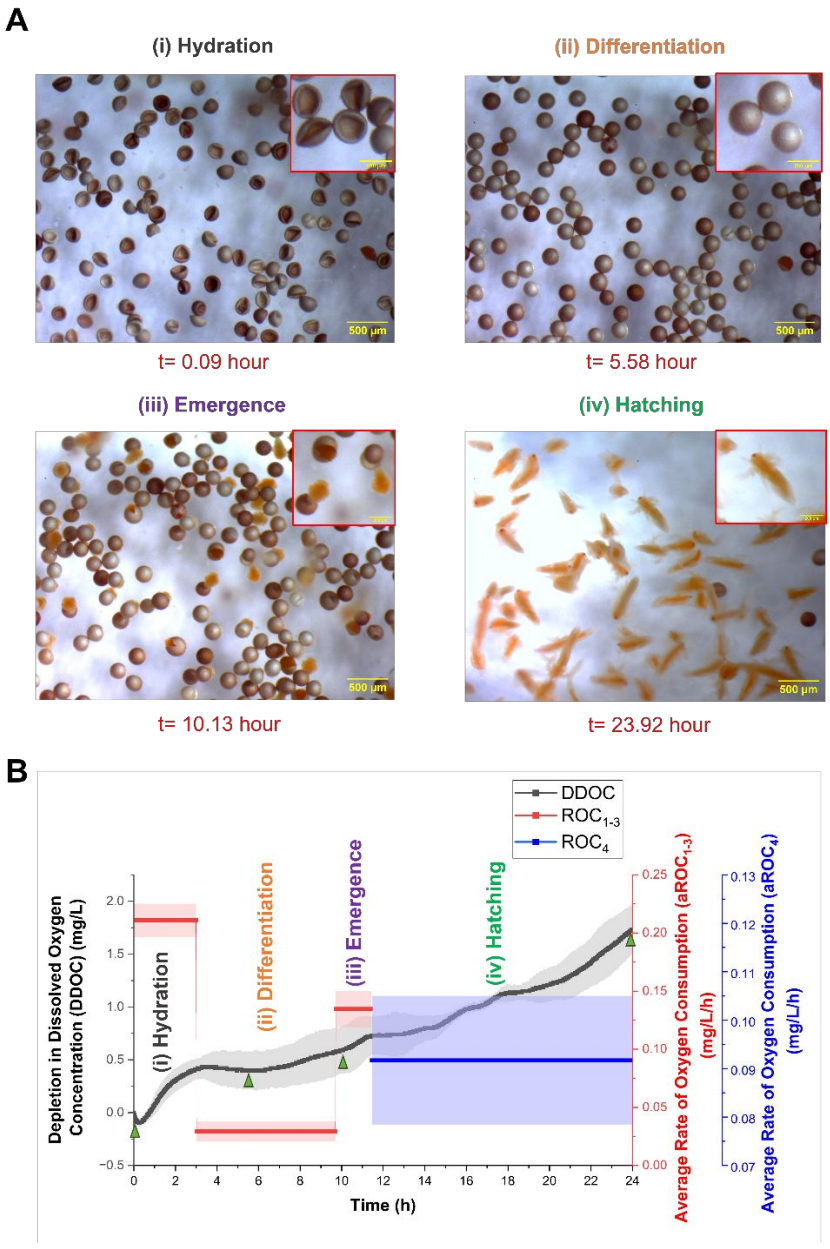

Figure 1. Photomicrographs and O_2 sensor data of the four stages of hatching process. (A) Photomicrographs at different hatching stages (scale bar = 500 µm) [the inset depicts the morphology of the cysts and nauplii (scale bar= 200 µm)]. (B) Depletion in dissolved oxygen concentration (DDOC) and average rate of oxygen consumption (aROC) of *Artemia* cysts during hatching without NPs (control) measured using on-chip sensors. (Bold lines represent averages with shaded regions showing SD (triplicate or more experiments at each NP condition). The black line/shaded area corresponds to DDOC, the red to $aROC_{1\text{-}3}$ (aROC of any of the 1st three stages of hatching), the blue to $aROC_4$ (aROC of any of the hatching stage), and green triangles in Figure 1B indicate DDOC at corresponding Figure 1A time points.)

The hatching process of *Artemia* consists of four distinct stages, encompassing the encysted state to swimming nauplii (91). Figure 1 illustrates photomicrographs of hatching cysts' morphological changes at different stages (Figure 1A) and corresponding oxygen consumption (Figure 1B) while not exposed to NPs (control). In addition to physical change, each hatching stage can be identified by energy metabolism (91–93), which is directly related to oxygen consumption and quantified by DDOC via an on-chip oxygen sensor (Text S3, SI) (Figure 1B). Figure 1B also depicts the aROC for each stage. Hydration stage (1st stage) initiates when a dormant cyst is immersed in saltwater at favorable conditions (62), causing it to absorb water through osmosis and shift from a cup-shaped to a nearly spherical form [Figure 1A(i)] (94). Cellular energy metabolism is then reactivated along with RNA and protein synthesis (92,95), resulting in an increase in aROC [Figure 1B(i)] (62). During differentiation (2nd stage), the spherical shape of the hatching cysts remains unchanged [Figure 1A(ii)] and there is no internal cell division or DNA replication (92,95) leading to an unchanged oxygen demand and a lower aROC [Figure 1B(ii)] (62). During emergence (3rd stage), the embryos emerge from the cysts [Figure 1A(iii)] due to increasing internal turgor pressure from glycerol synthesis (93), demanding more energy, and elevating aROC [Figure 1B(iii)] (62). Finally, during hatching stage (4th stage), embryos leave the cyst shells within a hatching membrane and start swimming [Figure 1A(iv)], expending energy for swimming activity, but requiring less oxygen than during emergence, resulting in a reduced aROC compared to that stage [Figure 1B(iv)] (62).

Understanding cyst-NPs interaction during hatching is critical, as penetration of NPs into cyst shell fracture and interior 3D porous structure (Figure S3, SI) can disrupt the hatching process. Since both PS and Ag NPs aggregated in saltwater (Figure S1, SI), it is also critical to understand how NP aggregates interact with cysts during hatching. These interactions were observed by SEM

imaging (Figure S4, SI) of cysts hatched in varying sizes of PS and Ag NP and MP suspensions in DIW, as briefly mentioned in Section 2 and elaborated in Text S2, SI. SEM images revealed that NP and MPs of varying size penetrated these cysts through cracks formed during cyst expansion/emergence due to hydration and internal turgor pressure. This penetration was facilitated further by the cysts' 3D honeycomb structure as evidenced through a comparison of cysts hatched in NP-mixed DIW with non-visible interior pores [Figure S4(B), SI] and those hatched in DIW alone, which exhibited void shell pores. Due to physical interaction between NPs and functional groups on cyst surfaces (96), such as amide, carboxylic, etc., the cysts were covered by NPs [Figure S4(C), SI]. Ag NPs were also found on cysts' inner porous structures by EDS [Figure S4(D), SI]. As PS NPs grow in size [in average, 1502.67 to 2558.67 nm in 1 h, depending on the NP concentration (see Figure S1(C), SI)], their infiltration capacity into the 3D inner porous structure (maximum pore size ~ 900 nm) decreases [Figure S4(B), SI]. We note that, the sizes of the Ag NPs utilized in this study (40 and 100 nm) are significantly smaller in size than the scale of the images presented in Figure S4(B-v) and Figure S4(B-vi) [scale bar= 1 μm]; these images simply demonstrate how the pores of the cysts are obscured as a result of the NPs penetrating the pores. In contrast, the EDS analysis (scale bar = 200 nm) [Figure S4(D), SI] reveals the uniform distribution of Ag NPs (initial size = 40 nm) on the interior surface of the cysts.

3.3 Effect of PS and Ag nanoparticles on the duration of different hatching stages and hatching rate

Figure 2A summarizes how PS and Ag NPs impact the duration of hatching stages. Overall, PS or Ag NPs have different effects on hatching stage durations and oxygen consumption depending on the particle concentration. This is in line with size-dependent toxicity (97) and changes in NP

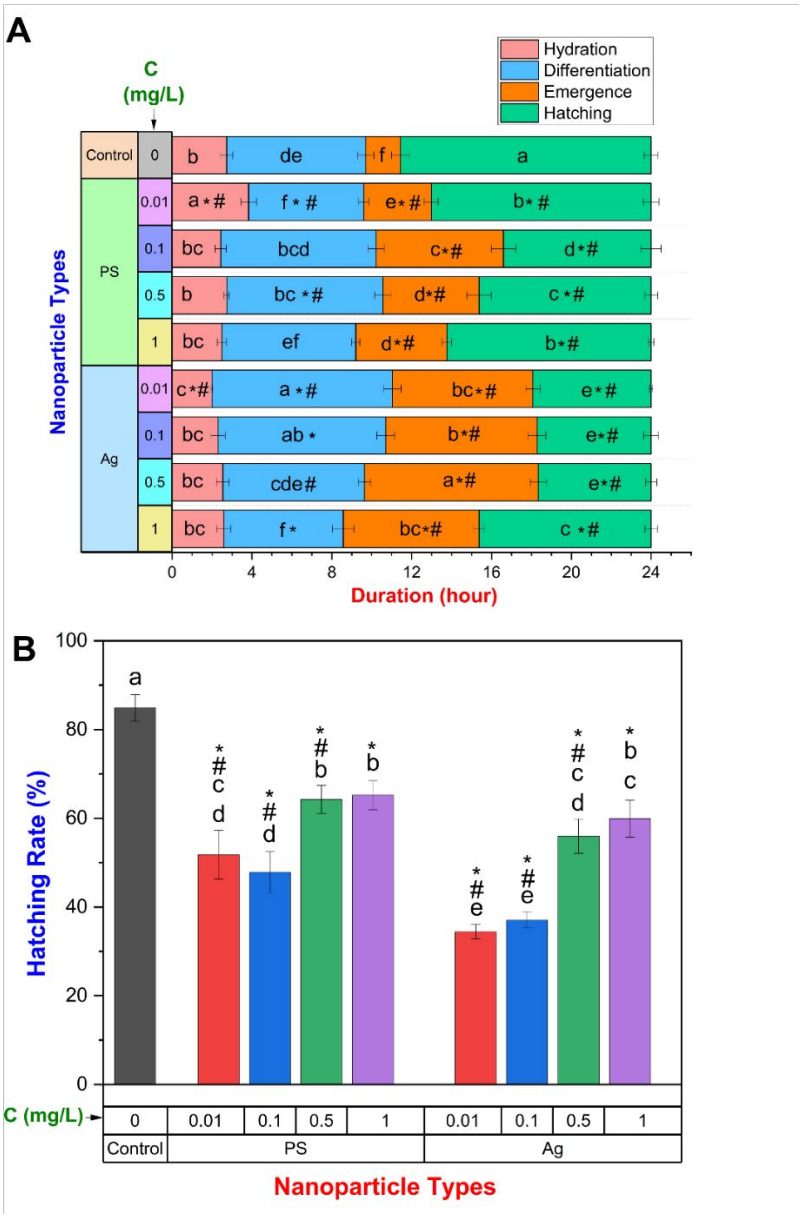

Figure 2. Effects of varying PS and Ag NP concentrations on- (A) durations of different hatching stages and (B) hatching rates. Data: mean ± SD (triplicate or more experiments at each NP condition). Statistically significant differences (p<0.05) denoted by distinct letters [within each stage in Figure 2(A)]. * and # highlight significant differences compared to control and the two NP treatments (PS and Ag) at the same concentration, respectively. "C" indicates NP concentrations.

aggregate size over time, which are affected by particle type and concentration, as shown in our study (Figure S1, SI).

The hydration stage is significantly affected (Figure 2A, red bars) only at the lowest concentration (0.01 mg/L) for both NP types. Lower concentrations allow NPs to penetrate fractures formed during hydration (Figure S4, SI), disrupting the osmotic gradient and impeding water absorption. The lack of significant impact of NPs at higher concentrations on hydration duration may be attributed to the increased aggregation of NPs in ASW at higher concentrations within a very brief period of time [Figure S1(C), SI]; such that these NPs were unable to penetrate the pores of the cyst interior, as described in section 3.2. While the simulation of cyst hatching with large PS particles indicated that larger aggregates could adhere to the cyst surface [Figure S4(C)], this was likely not as detrimental to the hydration process as the penetration of NPs into the cysts, which occurred easily at lower NP concentrations. Variations in hydration duration between the two NP types may relate to their differential toxicity (Section 3.5).

In the differentiation stage (Figure 2A, blue bars), NP type and concentration exert distinct effects. With PS NPs, differentiation stage duration initially dropped at the lowest concentration, then fluctuated with rising NP concentrations. In contrast, the impact of Ag NPs was greater, as the duration increased at the lowest concentration, but decreased with increasing NP concentrations. During differentiation, as cysts progress to the emergence stage, their shells fracture due to increasing turgor pressure. NPs may penetrate these fracturing cysts (Figure S4, SI), disrupting cellular differentiation and potentially causing genetic damage (98), thus elongating differentiation stage duration as compared to the control. The reduction in effects at higher NP concentrations was likely due to lower bioavailability from aggregation induced sedimentation (Figure S1), in line with previous NP studies (99) [90.] Nevertheless, we note that the presence of PS and Ag NPs at concentrations of 0.01 and 1 mg/L, respectively, resulted in a significantly reduced duration of the differentiation stage compared to the control, necessitating further investigation.

Both NP types significantly extended the emergence stage at all tested concentrations (Figure 2A, orange bars). This may result from NPs causing a bicarbonate ion deficit, impacting cytoplasmic membrane transport, and reducing osmotic potential (101). In this case, the cyst shell would break, but the inner cuticular membrane's elasticity would hinder emergence, prolonging the process (101). Notably, Ag NPs have a more significant effect on emergence duration compared to PS NPs. Being a heavy metal, this could be attributed to their higher toxicity. Previously, it has been shown that when *Ochromonas danica*, a type of algae, was exposed to both PS NPs and Ag NPs, the presence of Ag NPs resulted in a significantly higher inhibition of cell growth rate compared to the presence of PS NPs (102). In addition, another study conducted on *Danio rerio* (zebrafish) involved their exposure to both PS and the heavy metal Cadmium (Cd) (103). The Cd exposure led to greater growth suppression, decreased activity of antioxidant enzymes (e.g., superoxide dismutase, catalase, and glutathione peroxidase), elevated levels of reactive oxygen species, and tissue damage, in comparison to the PS exposure.

Finally, the hatching stage duration is the remaining time after the first three stages within the 24 hours of the experiment (Figure 2A-green bars). Cumulatively, both NPs significantly altered the durations of the hydration, differentiation, and emergence stages, affecting the time for the hatching stage. Specifically, the hatching stage was significantly shorter in the presence of Ag NPs compared to PS NPs and the control.

Figure 2B demonstrates the *Artemia* cyst hatching rates (HR) with PS and Ag NPs after 24 hours (calculated using Equation 3, SI). Previously, we demonstrated correlation of hatching duration with hatching rate (62). Both NP types inhibited hatching, but at higher concentrations, the effect decreased, resulting in a higher HR, consistent with duration findings (Figure 2A). The observed phenomenon may be attributed to the increased aggregation of NPs in ASW as the concentration

increases, as illustrated in Figure S1. This leads to a decrease in the bioavailability of the NPs due to their sedimentation. A similar reduction in toxicity with reduced bioavailability was observed when marine microalgae *Chlorella sp.* was exposed to TiO_2 NPs (99). The hatching chip material, polydimethylsiloxane (PDMS), has been extensively used in microfluidic devices for its excellent transparency, biocompatibility, and easy moldability (104,105). However, the bioavailability of NPs may be also influenced by the adsorption of NPs on PDMS surface (106), with a potential increase at higher NP concentration. Furthermore, the use of a very small volume (~563 μL) of the NP suspension in the hatching experiment on a hatching chip with a large surface area could amplify this impact. Hence, the underlying mechanisms of the observed decrease in toxic effects on the hatchability with increasing NP concentration in this study need further investigation. Overall, Ag NPs inhibited hatching more than PS NPs, except at the highest concentration of 1 mg/L, where HR was not significantly different. The lowest hatchability (34.42 ± 1.66%) was observed at 0.01 mg/L Ag NPs, 59.44% lower than the control. This mirrors the effects on different stage durations (Figure 5A), where Ag NPs had a more pronounced impact than PS NPs on hatching stages, notably the emergence stage, and hence had a confounding impact on the remaining time for the hatching stage during the 24 h of experiments. Specifically, interference with cellular differentiative process (98), reactive oxygen species (ROS) formation (107), damage in DNA moieties (108), cuticle damage (109), and perturbed osmotic gradient (110,111) may have contributed to the low hatching rate.

3.4 Effect of PS and Ag nanoparticles on oxygen consumption

The overall rate of oxygen consumption (oROC) demonstrated an ascending trend with the increase in both PS and Ag NP concentrations, in comparison to the control group (Figure 3A). Notably, there was a significant increase from an average oROC of 1.45×10^{-5} at the control to

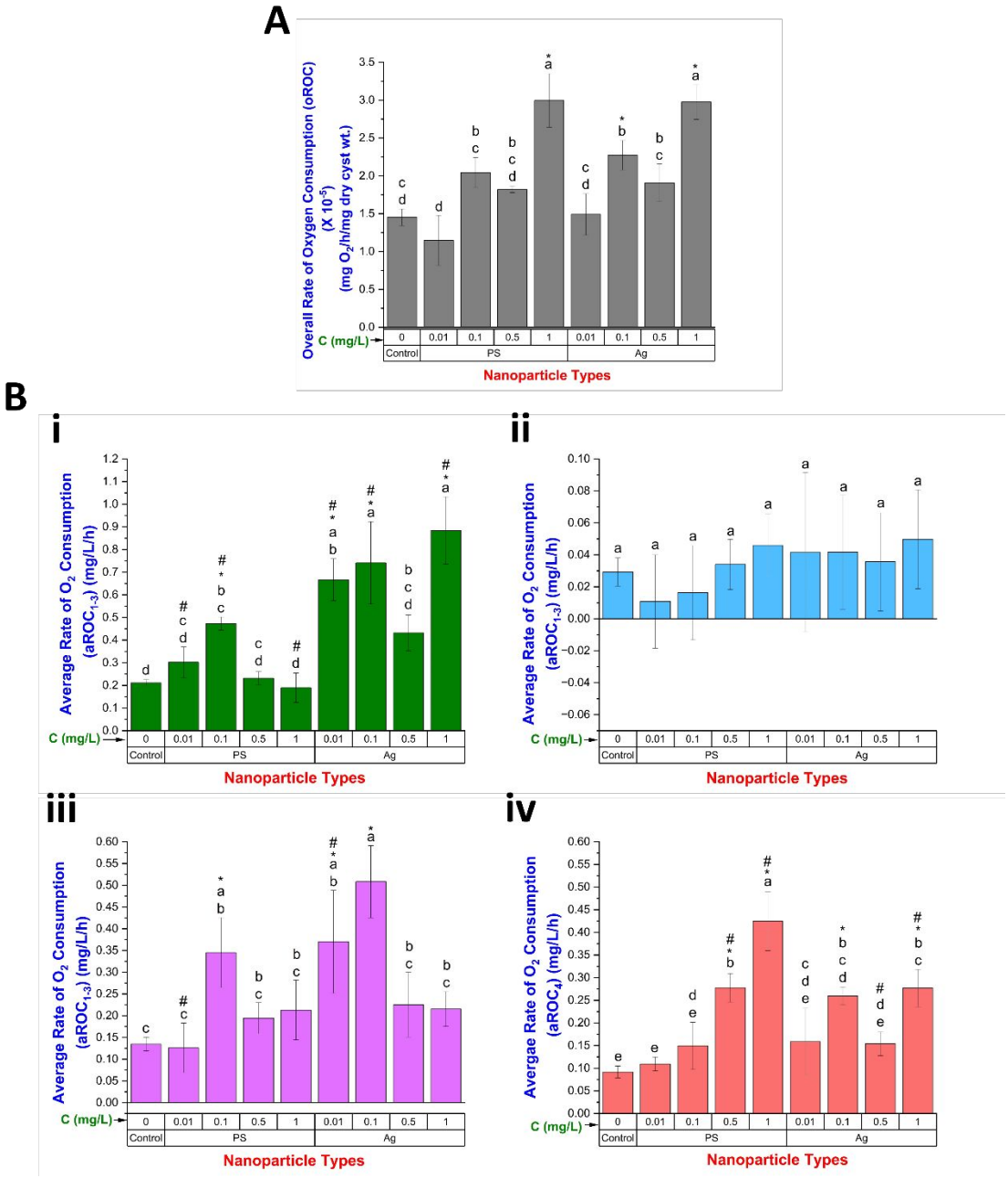

Figure 3. Effect of varying PS and Ag NP concentrations on *Artemia* oxygen consumption. (A) Overall rate of oxygen consumption (oROC) normalized based on the 24 h of hatching experiments and weight of initial dry cysts. (B) Average rate of oxygen consumption (aROC) during pre-hatching stages [(i) hydration, (ii) differentiation, (iii) emergence] normalized by stage duration and hatching rate (HR)% and (iv) hatching stage normalized by stage duration, HR%, and fraction of live *Artemia* (FLA). Data: mean ± SD (triplicate or more experiments at each NP condition). Distinct letters indicate statistical differences within each data category. Significantly different data from control is marked with "*", and at the same concentration under PS, and Ag treatments is marked with "#". "C" represents NP concentrations.

2.99×10^{-5} and 2.98×10^{-5} mg O_2/h/mg dry cyst wt. at a concentration of 1 mg/L for PS and Ag NP, respectively.

Upon examining the individual hatching stage, it was observed that the hydration stage [Figure 3B(i)] showed a significant increase in oxygen consumption with Ag NPs at all concentrations, except 0.5 mg/L, compared to the control. Conversely, PS NPs had no significant impact, except at 0.1 mg/L. While NPs didn't notably affect hydration duration (except at 0.01 mg/L) (Figure 5A-red bars), the observed increase in oxygen consumption might potentially compensate for insignificant net change in hydration duration. During differentiation [Figure 3B(ii)], oxygen consumption remained relatively constant, despite longer durations in NP presence (Figure 2A-blue bars), showing no significant change in aROC compared to the control, in line with our previous study (62). With delayed emergence in NP presence (Figure 2A-orange bars), the aROC during the emergence stage rose dramatically when PS NP concentration increased to 0.1 mg/L, but not further [Figure 3B(iii)]. As Ag NPs concentration climbed to 0.1 mg/L, the aROC increased and then decreased. Hatching stage oxygen consumption ($aROC_4$), which incorporated FLA alongside HR unlike the previous hatching stages, as mentioned in Text S3, SI, increased significantly at higher PS and Ag (except at 0.5 mg/L) NP concentrations. The elevated oxygen consumption seen during hatching suggests that the cysts experience a greater metabolic burden to successfully complete the hatching process, likely due to the toxic effects of the NPs. The increased need for oxygen after hatching (during nauplii stage) may be attributed to the gill damage characterized by hypertrophy and hyperplasia, and mitochondrial-rich cell (MRC) proliferation due to NP accumulation (112). Gill structure damage can compromise respiratory gas exchange, increase energy demand for osmoregulation, and subsequently elevate oxygen consumption (112,113). Similar oxygen consumption increase was reported in other aquatic species exposed to

different NPs, e.g., *Perca fluviatilis* exposed to $AgNO_3$ (114), *Brachidontes pharaonic* exposed to Ag NPs (115), *Fundulus heteroclitus* exposed to Cu NPs (116) and *Apistogramma agassizii* and *Paracheirodon axelrodi* exposed to Cu and CuO NPs (112).

3.5 Bioaccumulation of PS and Ag nanoparticles, acute toxicity, and swimming speed alteration

In newly hatched nauplii (Instar I), the inability to consume food or ingest nanoparticles is due to underdeveloped mouths and anuses (117). Nonetheless, NPs can be absorbed on their body surface and gills (118), negatively affecting metabolism and development. The transformation of *Artemia* nauplii Instar I into Instar II depends on temperature (119). At higher temperatures the transformation begins within an estimated time frame of 6-8 h (120–122). Upon hatching, all nauplii successfully complete this process within 24 h (119,123,124) and commence food ingestion via antennae sieving. However, this duration may also vary based on the strains of *Artemia* found in different regions, considering the variation in time required for their embryonic development (119). *Artemia* are nonselective filter feeders capable of consuming particles smaller than 50 μm (58), and the observed hatching stage duration of 7.74 to 12.56 h in this study under different NP exposures (Figure 2A) allowed time for beginning of this transformation. Figure 4 presents fluorescence and bright-field images of Instar II *Artemia* nauplii hatched in various NP concentrations. While Ag NPs are not fluorescent, they were imaged in bright field. *Artemia* ingested a substantial quantity of NPs, primarily accumulating in their digestive tract [Figure 4(B&D)]. Increased red fluorescence intensity (Figure 4B) indicates concentration-dependent NP uptake in the instar II stage of *Artemia* (Figure S7, SI). Bright-field images show empty digestive tracts in the control group (Figure 4C), while Ag NP-exposed *Artemia* exhibit dark areas, outlined by red arrows, indicating Ag NP presence (Figure 4D). Fluorescence images also reveal NP

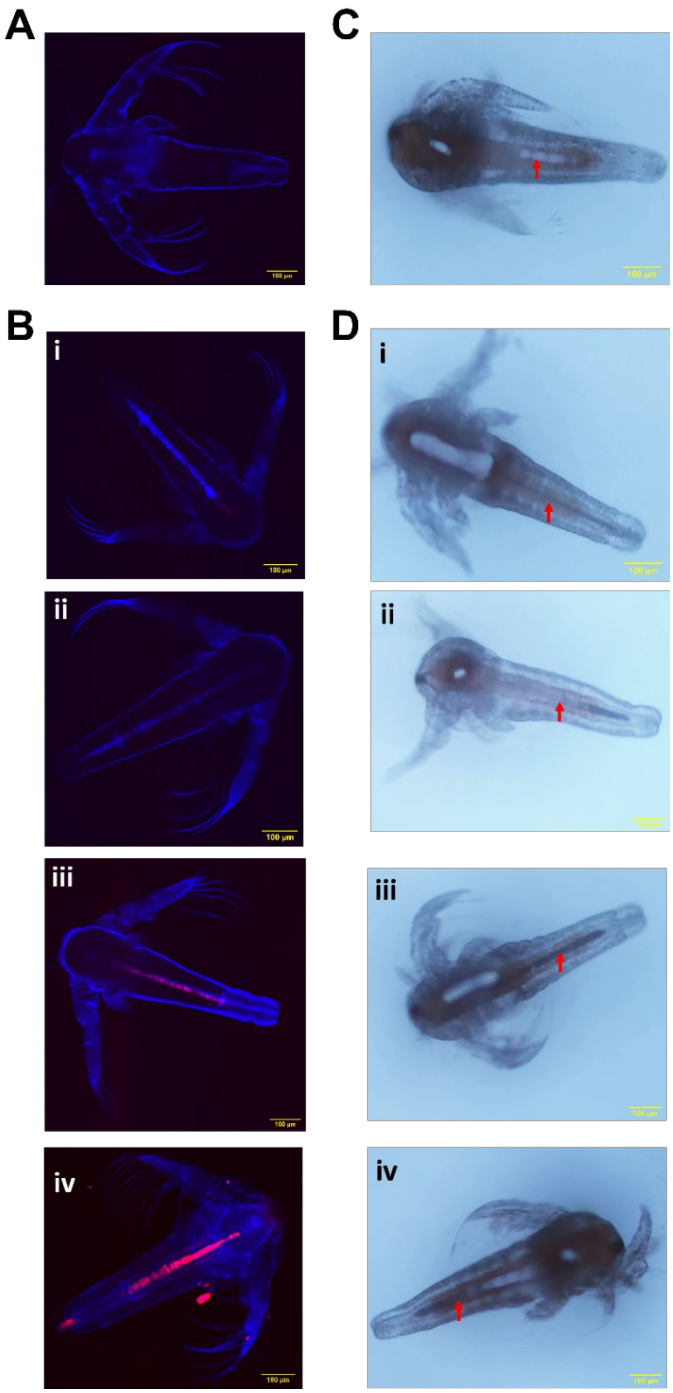

Figure 4. Fluorescence and bright-field microscopy images of *Artemia* nauplii after hatching in different nanoparticle conditions for 24 h. Figures 4A and 4C represent fluorescence and bright-field microscopy of control group (no NP). In Figures 4B (PS-fluorescence) and 4D (Ag-bright-field), i, ii, iii, and iv depict 0.01, 0.1, 0.5, and 1 mg/L NP concentrations, with red arrows indicating the digestive tract (scale bar= 100 µm).

aggregates on nauplii surfaces, especially at higher concentrations [Figure 4B(iv)]. However, this couldn't be confirmed via bright field microscopy for the Ag NPs.

Figure 5 displays the mortality rate and swimming speed alteration (SSA) of *Artemia* hatched with PS and Ag NPs over 24 hours. Figure 5A demonstrates that when NP concentrations increased, the mortality rate increased, which was the opposite of the trend observed in the hatching rate. This could be due to the NPs' reduced bioavailability during hatching due to aggregation, sedimentation, and probable adsorption by the PDMS, while their bioavailability increased after hatching, as the free-swimming *Artemia* may be more exposed to NP aggregates, via NP aggregate ingestion (Figure 4), particularly at the second instar stage when they have an open mouth and even through direct contact with the external surface (125). NP uptake, can impair digestive tract (55,58,126), infiltrate body tissues (118,127), increase reactive oxygen species (55,128,129), reduce body defense mechanisms (55,56), and cause tissue (58), DNA and mitochondrial damage (58,118), contributing to mortality. At the maximum NP concentration (1 mg/L), *Artemia* mortality for PS and Ag NPs was 28.47 ± 3.41% and 40.66 ± 4.48%, respectively, comparable with literature (52,53,58). Ag NPs exhibited higher toxicity, aligning with studies (130,131) indicating poorer gut health, increased oxidative stress, and DNA damage caused by Ag compared to PS, which could be due to the release of different Ag ions from Ag NPs (132,133), especially at higher salinities (57). Depending on the redox state of the ions, they adsorb on the *Artemia* cuticle structural component, chitin, via physisorption, causing significant cellular deformation (125). Among these, Ag^{3+} was reported to have higher interaction energy with chitin (125). Ag ions also interact with biomolecules found within cells, such as nucleic acid (134).

Besides mortality, NPs significantly altered *Artemia*'s swimming speed, measured by swimming speed alteration (SSA) (Figure 5B). Overall, positive SSA indicated significantly slower

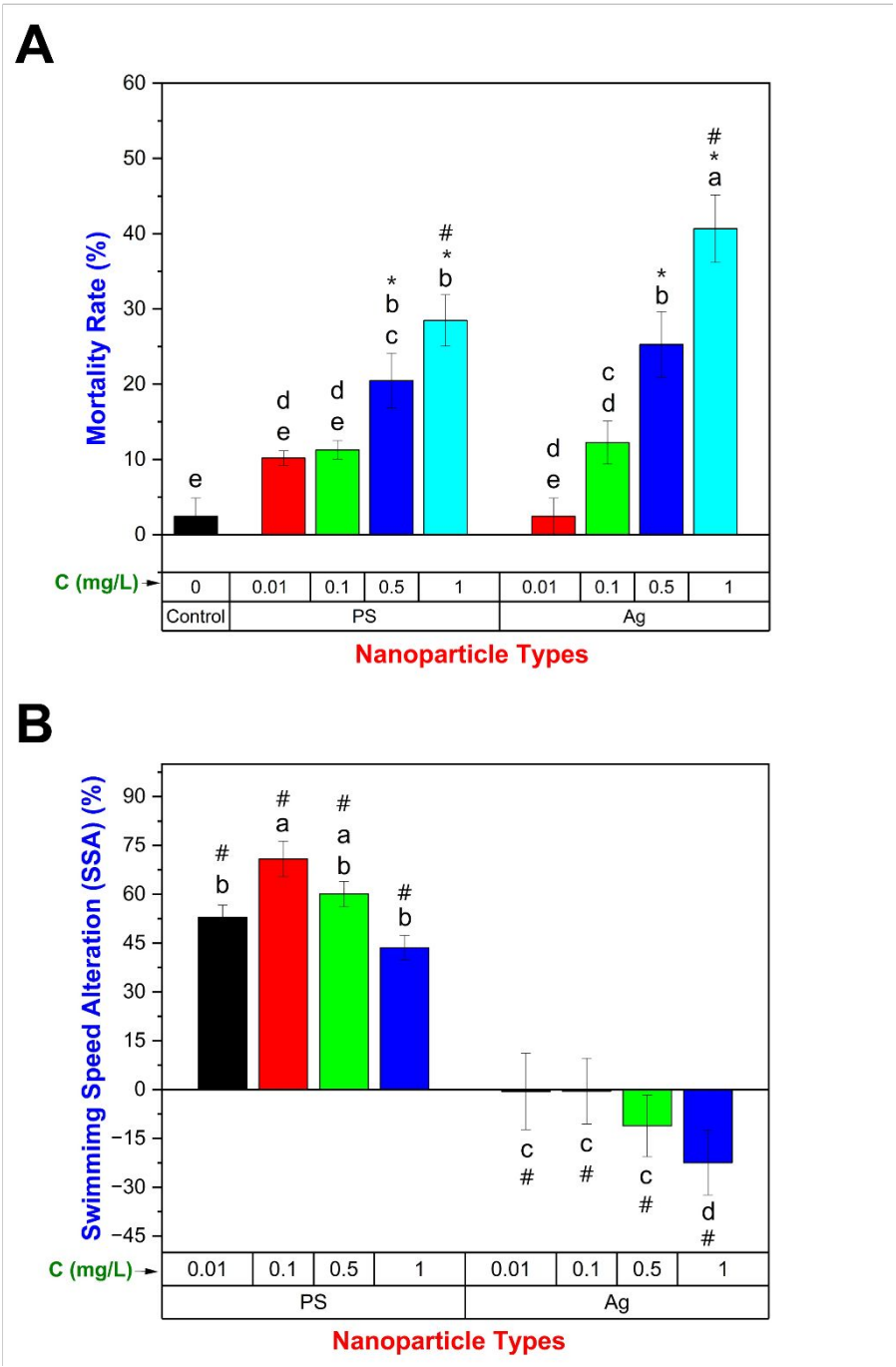

Figure 5. Effect of nanoparticle concentrations on hatched *Artemia* based on-(A) Mortality rate and (B) swimming speed alteration. Values were presented as mean ± SD (triplicate or more experiments at each NP condition). Distinct letters indicate statistical differences within each data category. Significantly different data from control is marked with "*", and at the same concentration under PS, and Ag treatments is marked with "#". "C" represents nanoparticle concentrations.

swimming compared to the control, similar to other marine animals exposed to PS NPs (135–138). However, with PS NP concentration higher than 0.1 mg/L, swimming speed comparatively increased, leading to a decreased SSA value with concentration. In contrast, swimming speed increased with Ag NP concentration, leading to a more negative SSA. Reduced swimming (positive SSA) may signal a protective response to stressors (e.g., environmental (139), oxidative stress (138,140), etc.) and impairments (e.g., visual (141), neuromotor deficits (142), etc.). Conversely, increased swimming speed (negative SSA) may indicate escape reactions from hazardous environments (139,143), psychostimulant action, or anxiety-like behavior (142). With greater acute toxicity (Figure 5A), Ag NP stimulated more to compensate for a homeostasis imbalance (144), encouraged faster swimming to escape a dangerous environment (143), or caused hyperactivity as observed in aquatic invertebrate larvae, including *Daphnia magna* (145).

3.6 Multivariate analysis

In a multivariate analysis, we explored associations between parameters involving hatching process and the nauplius stage, irrespective of NP type and concentration, categorized as pre-hatching and post-hatching (Figure S8, SI).

Hydration stage duration was negatively correlated with durations of differentiation and emergence stages but positively with the hatching stage. Differentiation and emergence stages extended at low NP concentrations and shortened at higher ones (Figure 2) due to NP toxicity and aggregation. Very low NP concentrations led to longer hydration correlating with shorter differentiation and emergence, explaining negative correlations. As NP concentration increased, differentiation and emergence stages shortened, allowing more time for hatching within 24 hours. Hydration aROC negatively correlated with hydration and hatching stage durations but positively with emergence stage duration. Emergence stage aROC negatively correlated with hydration and

hatching and positively with differentiation and emergence durations. Hydration aROC positively correlated with emergence aROC. NPs prolonged differentiation and emergence but shortened hydration and hatching, increasing oxygen consumption during hydration and emergence, adversely affecting hatchability. Differentiation and emergence durations, hydration, and emergence aROCs negatively correlated with hatching rate, whereas a longer hatching stage positively related to higher hatching rates, in line with our previous study (62).

Post-hatching, NPs affected early-stage nauplii through acute toxicity and compromised swimming (Figure 5). Figure S8, SI showed correlations, including a positive link between hatching stage aROC and mortality rate, but no significant correlation with hatching rate. These results indicated NPs caused toxicity in newly hatched nauplii, reducing viability, and increasing oxygen demand. Conversely, SSA was associated only with hatching stage duration. PS NPs with longer hatching stages led to positive SSA, while Ag NPs with shorter hatching stages resulted in negative SSA.

4. Conclusion

This study investigated real-time oxygen consumption and morphological changes to understand the impact of various marine nanopollutants on the hatching process and early development of *Artemia,* a common zooplankton in ecotoxicology. In agreement with previous studies evaluating end point hatching rates, both NPs had detrimental impacts on the hatching performance (58–61). In this work, we were able to demonstrate a correlation between hatching stage progression and hatching rate. For example, dormant cysts that consumed less metabolic energy (lower oxygen consumption) in the hydration and emergence stages with less time needed for differentiation and emergence, leaving more time for hatching, had a higher hatchability. Throughout different stages of the hatching process and at the endpoint (hatching rate), a trend of diminishing toxicity with

increasing dosage was observed. However, the mortality rate increased dose-dependently, which is consistent with earlier studies (52,53,56,58,61). The observed phenomenon can be attributed to the increased NP aggregation, sedimentation, or adsorption by PDMS which decreases the bioavailability of NPs during hatching. After hatching, free-swimming *Artemia* nauplii became exposed to NP aggregates and likely Ag ions, and readily ingested aggregated NPs, increasing their bioavailability. Ag NPs had greater effects on hatchability and mortality rates than PS NPs, likely due to the higher toxicity of heavy metals (146,147), which was exacerbated by the interaction of their ions with the cuticle (125). In addition, while swimming speed increased with Ag NPs, it decreased with PS NPs, possibly due to varying coping mechanisms/effects in response to diverse environmental stimuli.

We anticipate that the controlled microfluidic environment developed here, coupled with integrated real-time sensing and microscopy could be used to advance the comprehensive assessment of a broad range of marine nanopollutants (nanoparticles, pesticides, fertilizers, detergents, sewage, industrial effluents, etc.), on biological processes and marine organisms ranging from zooplankton to fish larvae.

CRediT authorship contribution statement

Preyojon Dey: Conceptualization, Methodology, Investigation, Formal analysis, Visualization, Writing - Original Draft, Writing - Review & Editing **Terence M. Bradley:** Conceptualization, Supervision, Formal analysis, Writing - Review & Editing, Funding acquisition **Alicia Boymelgreen:** Conceptualization, Supervision, Formal analysis, Writing - Review & Editing, Funding acquisition.

Declaration of competing interest

There is no competing interest to declare.

Acknowledgments

This work is supported by the National Science Foundation (award number: 2038484, year: 2020) and FIU University Graduate School Dissertation Year Fellowship. This is contribution #1692 from the Institute of Environment at Florida International University. Graphs were plotted using OriginPro 2023 (https://www.originlab.com/). Schematics were created using Biorender (https://biorender.com/).

References

1. Avio CG, Gorbi S, Regoli F. Plastics and microplastics in the oceans: From emerging pollutants to emerged threat. Marine Environmental Research. 2017 Jul 1;128:2–11.

2. Jambeck JR, Geyer R, Wilcox C, Siegler TR, Perryman M, Andrady A, et al. Marine pollution. Plastic waste inputs from land into the ocean. Science. 2015 Feb 13;347(6223):768–71.

3. Auta HS, Emenike CU, Fauziah SH. Distribution and importance of microplastics in the marine environment: A review of the sources, fate, effects, and potential solutions. Environment International. 2017 May 1;102:165–76.

4. Verster C, Bouwman H. Land-based sources and pathways of marine plastics in a South African context. South African Journal of Science. 2020;116(5–6):1–9.

5. Ter Halle A, Ladirat L, Martignac M, Mingotaud AF, Boyron O, Perez E. To what extent are microplastics from the open ocean weathered? Environmental Pollution. 2017;227:167–74.

6. Andrady AL. Weathering and fragmentation of plastic debris in the ocean environment. Marine Pollution Bulletin. 2022;180:113761.

7. Kiran BR, Kopperi H, Venkata Mohan S. Micro/nano-plastics occurrence, identification, risk analysis and mitigation: challenges and perspectives. Rev Environ Sci Biotechnol. 2022;21(1):169–203.

8. Maharana D, Saha M, Dar JY, Rathore C, Sreepada RA, Xu XR, et al. Assessment of micro and macroplastics along the west coast of India: Abundance, distribution, polymer type and toxicity. Chemosphere. 2020 May 1;246:125708.

9. Mariano S, Tacconi S, Fidaleo M, Rossi M, Dini L. Micro and nanoplastics identification: classic methods and innovative detection techniques. Frontiers in toxicology. 2021;3:636640.

10. Servin AD, White JC. Nanotechnology in agriculture: next steps for understanding engineered nanoparticle exposure and risk. NanoImpact. 2016;1:9–12.

11. Khan S, Naushad M, Al-Gheethi A, Iqbal J. Engineered nanoparticles for removal of pollutants from wastewater: Current status and future prospects of nanotechnology for remediation strategies. Journal of Environmental Chemical Engineering. 2021;9(5):106160.

12. Lithner D, Larsson Å, Dave G. Environmental and health hazard ranking and assessment of plastic polymers based on chemical composition. Science of The Total Environment. 2011 Aug 15;409(18):3309–24.

13. Clayton CA, Walker TR, Bezerra JC, Adam I. Policy responses to reduce single-use plastic marine pollution in the Caribbean. Marine Pollution Bulletin. 2021 Jan 1;162:111833.

14. Turner A. Foamed Polystyrene in the Marine Environment: Sources, Additives, Transport, Behavior, and Impacts. Environ Sci Technol. 2020 Sep 1;54(17):10411–20.

15. Saido K, Koizumi K, Sato H, Ogawa N, Kwon BG, Chung SY, et al. New analytical method for the determination of styrene oligomers formed from polystyrene decomposition and its application at the coastlines of the North-West Pacific Ocean. Science of The Total Environment. 2014 Mar 1;473–474:490–5.

16. Hadrup N, Sharma AK, Loeschner K. Toxicity of silver ions, metallic silver, and silver nanoparticle materials after in vivo dermal and mucosal surface exposure: A review. Regulatory Toxicology and Pharmacology. 2018;98:257–67.

17. Kamat V, Dey P, Bodas D, Kaushik A, Boymelgreen A, Bhansali S. Active microfluidic reactor-assisted controlled synthesis of nanoparticles and related potential biomedical applications. J Mater Chem B [Internet]. 2023 May 9 [cited 2023 May 15]; Available from: https://pubs.rsc.org/en/content/articlelanding/2023/tb/d3tb00057e

18. Vance ME, Kuiken T, Vejerano EP, McGinnis SP, Hochella Jr MF, Rejeski D, et al. Nanotechnology in the real world: Redeveloping the nanomaterial consumer products inventory. Beilstein journal of nanotechnology. 2015;6(1):1769–80.

19. Radetić M. Functionalization of textile materials with silver nanoparticles. Journal of Materials Science. 2013;48:95–107.

20. Ratte HT. Bioaccumulation and toxicity of silver compounds: a review. Environmental toxicology and chemistry: an international journal. 1999;18(1):89–108.

21. Putri AR, Zamani NP, Bengen DG. Effect of microplastics and natural microparticles on green Mussel (Perna viridis). IOP Conf Ser: Earth Environ Sci. 2021 May;771(1):012008.

22. Masiá P, Ardura A, García-Vázquez E. Virgin polystyrene microparticles exposure leads to changes in gills DNA and physical condition in the Mediterranean mussel Mytilus galloprovincialis. Animals. 2021;11(8):2317.

23. Nunes B, Simões MI, Navarro JC, Castro BB. First ecotoxicological characterization of paraffin microparticles: a biomarker approach in a marine suspension-feeder, Mytilus sp. Environmental Science and Pollution Research. 2020;27:41946–60.

24. Messinetti S, Mercurio S, Parolini M, Sugni M, Pennati R. Effects of polystyrene microplastics on early stages of two marine invertebrates with different feeding strategies. Environmental Pollution. 2018;237:1080–7.

25. Larue C, Sarret G, Castillo-Michel H, Pradas del Real AE. A critical review on the impacts of nanoplastics and microplastics on aquatic and terrestrial photosynthetic organisms. Small. 2021;17(20):2005834.

26. Allen D, Allen S, Abbasi S, Baker A, Bergmann M, Brahney J, et al. Microplastics and nanoplastics in the marine-atmosphere environment. Nat Rev Earth Environ. 2022 Jun;3(6):393–405.

27. Zhang M, Xu L. Transport of micro- and nanoplastics in the environment: Trojan-Horse effect for organic contaminants. Critical Reviews in Environmental Science and Technology. 2022 Mar 4;52(5):810–46.

28. Sarasamma S, Audira G, Siregar P, Malhotra N, Lai YH, Liang ST, et al. Nanoplastics Cause Neurobehavioral Impairments, Reproductive and Oxidative Damages, and Biomarker Responses in Zebrafish: Throwing up Alarms of Wide Spread Health Risk of Exposure. International Journal of Molecular Sciences. 2020 Jan;21(4):1410.

29. Brandts I, Barría C, Martins MA, Franco-Martínez L, Barreto A, Tvarijonaviciute A, et al. Waterborne exposure of gilthead seabream (Sparus aurata) to polymethylmethacrylate nanoplastics causes effects at cellular and molecular levels. Journal of Hazardous Materials. 2021 Feb 5;403:123590.

30. Shen M, Zhang Y, Zhu Y, Song B, Zeng G, Hu D, et al. Recent advances in toxicological research of nanoplastics in the environment: A review. Environmental Pollution. 2019 Sep 1;252:511–21.

31. Al-Thawadi S. Microplastics and Nanoplastics in Aquatic Environments: Challenges and Threats to Aquatic Organisms. Arab J Sci Eng. 2020 Jun 1;45(6):4419–40.

32. Kumari P, Panda PK, Jha E, Kumari K, Nisha K, Mallick MA, et al. Mechanistic insight to ROS and apoptosis regulated cytotoxicity inferred by green synthesized CuO nanoparticles from Calotropis gigantea to embryonic zebrafish. Scientific reports. 2017;7(1):1–17.

33. Muller EB, Lin S, Nisbet RM. Quantitative Adverse Outcome Pathway Analysis of Hatching in Zebrafish with CuO Nanoparticles. Environ Sci Technol. 2015 Oct 6;49(19):11817–24.

34. Ross PM, Parker L, O'Connor WA, Bailey EA. The Impact of Ocean Acidification on Reproduction, Early Development and Settlement of Marine Organisms. Water. 2011 Dec;3(4):1005–30.

35. Ashjian CJ, Campbell RG, Welch HE, Butler M, Van Keuren D. Annual cycle in abundance, distribution, and size in relation to hydrography of important copepod species in the western Arctic Ocean. Deep Sea Research Part I: Oceanographic Research Papers. 2003 Oct 1;50(10):1235–61.

36. Griffitt RJ, Luo J, Gao J, Bonzongo JC, Barber DS. Effects of particle composition and species on toxicity of metallic nanomaterials in aquatic organisms. Environmental Toxicology and Chemistry. 2008;27(9):1972–8.

37. Exbrayat JM, Moudilou EN, Lapied E. Harmful effects of nanoparticles on animals. Journal of Nanotechnology. 2015;2015.

38. Worthen AJ, Tran V, Cornell KA, Truskett TM, Johnston KP. Steric stabilization of nanoparticles with grafted low molecular weight ligands in highly concentrated brines including divalent ions. Soft Matter. 2016;12(7):2025–39.

39. Chinnapongse SL, MacCuspie RI, Hackley VA. Persistence of singly dispersed silver nanoparticles in natural freshwaters, synthetic seawater, and simulated estuarine waters. Science of The Total Environment. 2011 May 15;409(12):2443–50.

40. Wang J, Zhao X, Wu F, Tang Z, Zhao T, Niu L, et al. Impact of montmorillonite clay on the homo- and heteroaggregation of titanium dioxide nanoparticles (nTiO2) in synthetic and natural waters. Science of The Total Environment. 2021 Aug 25;784:147019.

41. Angel BM, Batley GE, Jarolimek CV, Rogers NJ. The impact of size on the fate and toxicity of nanoparticulate silver in aquatic systems. Chemosphere. 2013 Sep 1;93(2):359–65.

42. Manfra L, Rotini A, Bergami E, Grassi G, Faleri C, Corsi I. Comparative ecotoxicity of polystyrene nanoparticles in natural seawater and reconstituted seawater using the rotifer Brachionus plicatilis. Ecotoxicology and environmental safety. 2017;145:557–63.

43. Chae YJ, Pham CH, Lee J, Bae E, Yi J, Gu MB. Evaluation of the toxic impact of silver nanoparticles on Japanese medaka (Oryzias latipes). Aquatic toxicology. 2009;94(4):320–7.

44. Rocha GS, Katan T, Parrish CC, Kurt Gamperl A. Effects of wild zooplankton versus enriched rotifers and Artemia on the biochemical composition of Atlantic cod (Gadus morhua) larvae. Aquaculture. 2017 Oct 1;479:100–13.

45. Camargo WN, Durán GC, Rada OC, Hernández LC, Linero JCG, Muelle IM, et al. Determination of biological and physicochemical parameters of Artemia franciscana strains in hypersaline environments for aquaculture in the Colombian Caribbean. Saline Systems. 2005 Oct 26;1(1):9.

46. Van Stappen G, Sui L, Hoa VN, Tamtin M, Nyonje B, de Medeiros Rocha R, et al. Review on integrated production of the brine shrimp Artemia in solar salt ponds. Reviews in Aquaculture. 2020;12(2):1054–71.

47. Gajardo GM, Beardmore JA. The brine shrimp Artemia: adapted to critical life conditions. Frontiers in physiology. 2012;185.

48. Vikas PA, Thomas PC, Sajeshkumar NK, Chakraborthy K, Sanil NK, Vijayan KK. Effect of salinity stress on biochemical constituents and ArHsp22 gene expression in Artemia franciscana. Indian J Fish [Internet]. 2016 Oct 7 [cited 2023 Mar 10];63(3). Available from: http://epubs.icar.org.in/ejournal/index.php/IJF/article/view/50894

49. Browne R, Wanigasekera G. Combined effects of salinity and temperature on survival and reproduction of five species of Artemia. Journal of experimental marine biology and ecology. 2000;244(1):29–44.

50. Johari SA, Rasmussen K, Gulumian M, Ghazi-Khansari M, Tetarazako N, Kashiwada S, et al. Introducing a new standardized nanomaterial environmental toxicity screening testing procedure,

ISO/TS 20787: aquatic toxicity assessment of manufactured nanomaterials in saltwater Lakes using Artemia sp. nauplii. Toxicology Mechanisms and Methods. 2019 Feb 12;29(2):95–109.

51. Bergami E, Bocci E, Vannuccini ML, Monopoli M, Salvati A, Dawson KA, et al. Nano-sized polystyrene affects feeding, behavior and physiology of brine shrimp Artemia franciscana larvae. Ecotoxicology and Environmental Safety. 2016 Jan 1;123:18–25.

52. Bergami E, Pugnalini S, Vannuccini ML, Manfra L, Faleri C, Savorelli F, et al. Long-term toxicity of surface-charged polystyrene nanoplastics to marine planktonic species Dunaliella tertiolecta and Artemia franciscana. Aquatic Toxicology. 2017 Aug 1;189:159–69.

53. Varó I, Perini A, Torreblanca A, Garcia Y, Bergami E, Vannuccini ML, et al. Time-dependent effects of polystyrene nanoparticles in brine shrimp Artemia franciscana at physiological, biochemical and molecular levels. Science of the Total Environment. 2019;675:570–80.

54. Machado AJT, Mataribu B, Serrão C, da Silva Silvestre L, Farias DF, Bergami E, et al. Single and combined toxicity of amino-functionalized polystyrene nanoparticles with potassium dichromate and copper sulfate on brine shrimp Artemia franciscana larvae. Environ Sci Pollut Res. 2021 Sep 1;28(33):45317–34.

55. An HJ, Sarkheil M, Park HS, Yu IJ, Johari SA. Comparative toxicity of silver nanoparticles (AgNPs) and silver nanowires (AgNWs) on saltwater microcrustacean, Artemia salina. Comparative Biochemistry and Physiology Part C: Toxicology & Pharmacology. 2019 Apr 1;218:62–9.

56. Demarchi CA, da Silva LM, Niedźwiecka A, Ślawska-Waniewska A, Lewińska S, Dal Magro J, et al. Nanoecotoxicology study of the response of magnetic O-Carboxymethylchitosan loaded silver nanoparticles on Artemia salina. Environmental Toxicology and Pharmacology. 2020 Feb 1;74:103298.

57. Asadi Dokht Lish R, Johari SA, Sarkheil M, Yu IJ. On how environmental and experimental conditions affect the results of aquatic nanotoxicology on brine shrimp (Artemia salina): A case of silver nanoparticles toxicity. Environmental Pollution. 2019 Dec 1;255:113358.

58. Arulvasu C, Jennifer SM, Prabhu D, Chandhirasekar D. Toxicity effect of silver nanoparticles in brine shrimp Artemia. The Scientific World Journal. 2014;2014.

59. Rekulapally R, Murthy Chavali LN, Idris MM, Singh S. Toxicity of TiO2, SiO2, ZnO, CuO, Au and Ag engineered nanoparticles on hatching and early nauplii of Artemia sp. PeerJ. 2019 Jan 3;6:e6138.

60. Pecoraro R, Scalisi EM, Messina G, Fragalà G, Ignoto S, Salvaggio A, et al. Artemia salina: A microcrustacean to assess engineered nanoparticles toxicity. Microscopy Research and Technique. 2021;84(3):531–6.

61. Kos M, Kahru A, Drobne D, Singh S, Kalčíková G, Kühnel D, et al. A case study to optimise and validate the brine shrimp Artemia franciscana immobilisation assay with silver nanoparticles: The role of harmonisation. Environmental Pollution. 2016 Jun 1;213:173–83.

62. Dey P, Bradley TM, Boymelgreen A. The impact of selected abiotic factors on Artemia hatching process through real-time observation of oxygen changes in a microfluidic platform. Sci Rep. 2023 Apr 19;13(1):6370.

63. Krenger R, Cornaglia M, Lehnert T, Gijs MA. Microfluidic system for Caenorhabditis elegans culture and oxygen consumption rate measurements. Lab on a Chip. 2020;20(1):126–35.

64. Rahman M, Edwards H, Birze N, Gabrilska R, Rumbaugh KP, Blawzdziewicz J, et al. NemaLife chip: a micropillar-based microfluidic culture device optimized for aging studies in crawling C. elegans. Scientific reports. 2020;10(1):1–19.

65. Mondal S, Hegarty E, Martin C, Gökçe SK, Ghorashian N, Ben-Yakar A. Large-scale microfluidics providing high-resolution and high-throughput screening of Caenorhabditis elegans poly-glutamine aggregation model. Nature communications. 2016;7(1):1–11.

66. Akagi J, Khoshmanesh K, Hall CJ, Cooper JM, Crosier KE, Crosier PS, et al. Fish on chips: Microfluidic living embryo array for accelerated in vivo angiogenesis assays. Sensors and Actuators B: Chemical. 2013;189:11–20.

67. Akagi J, Khoshmanesh K, Hall CJ, Crosier KE, Crosier PS, Cooper JM, et al. Fish on chips: automated microfluidic living embryo arrays. Procedia Engineering. 2012;47:84–7.

68. Yang F, Gao C, Wang P, Zhang GJ, Chen Z. Fish-on-a-chip: microfluidics for zebrafish research. Lab Chip. 2016 Mar 23;16(7):1106–25.

69. Cheung S, Cheung RY. Effects of heavy metals on oxygen consumption and ammonia excretion in green-lipped mussels (Perna viridis). Marine Pollution Bulletin. 1995;31(4–12):381–6.

70. Alessi C, Giomi F, Furnari F, Sarà G, Chemello R, Milazzo M. Ocean acidification and elevated temperature negatively affect recruitment, oxygen consumption and calcification of the reef-building Dendropoma cristatum early life stages: Evidence from a manipulative field study. Science of The Total Environment. 2019;693:133476.

71. Baden SP. Oxygen consumption rate of shrimp exposed to crude oil extract. Marine Pollution Bulletin. 1982;13(7):230–3.

72. C. Lasave L, M. Borisov S, Ehgartner J, Mayr T. Quick and simple integration of optical oxygen sensors into glass-based microfluidic devices. RSC Advances. 2015;5(87):70808–16.

73. Curto VF, Coyle S, Byrne R, Angelov N, Diamond D, Benito-Lopez F. Concept and development of an autonomous wearable micro-fluidic platform for real time pH sweat analysis. Sensors and Actuators B: Chemical. 2012 Dec 1;175:263–70.

74. Qiu W, Nagl S. Automated Miniaturized Digital Microfluidic Antimicrobial Susceptibility Test Using a Chip-Integrated Optical Oxygen Sensor. ACS Sens. 2021 Mar 26;6(3):1147–56.

75. Li Z, Dey P, Kim SJ. Microfluidic single valve oscillator for blood plasma filtration. Sensors and Actuators B: Chemical. 2019;296:126692.

76. Dey P, Li Z, Kim SJ. Pulsatile microfluidic blood plasma filtration chip. 대한기계학회 춘추학술대회. 2019;1458–60.

77. Ahamed MdA, Kim G, Li Z, Kim SJ. Pre-programmed microdroplet generator to control wide-ranging chemical concentrations. Analytica Chimica Acta. 2022 Dec 15;1236:340587.

78. Reisser J, Shaw J, Wilcox C, Hardesty BD, Proietti M, Thums M, et al. Marine Plastic Pollution in Waters around Australia: Characteristics, Concentrations, and Pathways. PLOS ONE. 2013 Nov 27;8(11):e80466.

79. Law KL. Plastics in the Marine Environment. Annual Review of Marine Science. 2017;9(1):205–29.

80. Kim L, Cui R, Kwak JI, An YJ. Sub-acute exposure to nanoplastics via two-chain trophic transfer: From brine shrimp Artemia franciscana to small yellow croaker Larimichthys polyactis. Marine Pollution Bulletin. 2022;175:113314.

81. Gambardella C, Mesarič T, Milivojević T, Sepčić K, Gallus L, Carbone S, et al. Effects of selected metal oxide nanoparticles on Artemia salina larvae: evaluation of mortality and behavioural and biochemical responses. Environ Monit Assess. 2014 Jul 1;186(7):4249–59.

82. Mesarič T, Gambardella C, Milivojević T, Faimali M, Drobne D, Falugi C, et al. High surface adsorption properties of carbon-based nanomaterials are responsible for mortality, swimming inhibition, and biochemical responses in Artemia salina larvae. Aquatic Toxicology. 2015;163:121–9.

83. Wang Q, Duan X, Huang F, Cheng H, Zhang C, Li L, et al. Polystyrene nanoplastics alter virus replication in orange-spotted grouper (Epinephelus coioides) spleen and brain tissues and spleen cells. Journal of Hazardous Materials. 2021;416:125918.

84. Singhal P, Pulhani V, Ali SM, Ningthoujam RS. Sorption of different metal ions on magnetic nanoparticles and their effect on nanoparticles settlement. Environmental Nanotechnology, Monitoring & Management. 2019;11:100202.

85. Dutta A, Paul A, Chattopadhyay A. The effect of temperature on the aggregation kinetics of partially bare gold nanoparticles. RSC advances. 2016;6(85):82138–49.

86. Abdelmonem AM, Pelaz B, Kantner K, Bigall NC, del Pino P, Parak WJ. Charge and agglomeration dependent in vitro uptake and cytotoxicity of zinc oxide nanoparticles. Journal of Inorganic Biochemistry. 2015 Dec 1;153:334–8.

87. Halamoda-Kenzaoui B, Ceridono M, Urbán P, Bogni A, Ponti J, Gioria S, et al. The agglomeration state of nanoparticles can influence the mechanism of their cellular internalisation. Journal of Nanobiotechnology. 2017 Jun 26;15(1):48.

88. Prathna TC, Chandrasekaran N, Mukherjee A. Studies on aggregation behaviour of silver nanoparticles in aqueous matrices: Effect of surface functionalization and matrix composition. Colloids and Surfaces A: Physicochemical and Engineering Aspects. 2011 Oct 20;390(1):216–24.

89. Wang H, Burgess RM, Cantwell MG, Portis LM, Perron MM, Wu F, et al. Stability and aggregation of silver and titanium dioxide nanoparticles in seawater: Role of salinity and dissolved organic carbon. Environmental Toxicology and Chemistry. 2014;33(5):1023–9.

90. Zhou D, Keller AA. Role of morphology in the aggregation kinetics of ZnO nanoparticles. Water Research. 2010 May 1;44(9):2948–56.

91. Emerson DN. Surface area respiration during the hatching of encysted embryos of the brine shrimp, Artemia salina. The Biological Bulletin. 1967;132(2):156–60.

92. Emerson D. The metabolism of hatching embryos of the brine shrimp Artemia salina. In 1963. p. 131–5.

93. Drinkwater LE, Crowe JH. Hydration state, metabolism, and hatching of Mono Lake Artemia cysts. The Biological Bulletin. 1991;180(3):432–9.

94. CLEGG JS. The control of emergence and metabolism by external osmotic pressure and the role of free glycerol in developing cysts of Artemia salina. Journal of Experimental Biology. 1964;41(4):879–92.

95. Clegg JS, Trotman CN. Physiological and biochemical aspects of Artemia ecology. In: Artemia: Basic and applied biology. Springer; 2002. p. 129–70.

96. Wang B, Xia J, Mei L, Wang L, Zhang Q. Highly Efficient and Rapid Lead(II) Scavenging by the Natural Artemia Cyst Shell with Unique Three-Dimensional Porous Structure and Strong Sorption Affinity. ACS Sustainable Chem Eng. 2018 Jan 2;6(1):1343–51.

97. Kögel T, Bjorøy Ø, Toto B, Bienfait AM, Sanden M. Micro-and nanoplastic toxicity on aquatic life: Determining factors. Science of the Total Environment. 2020;709:136050.

98. Migliore L, Civitareale C, Brambilla G, Delupis GDD. Toxicity of several important agricultural antibiotics to Artemia. Water Research. 1997 Jul 1;31(7):1801–6.

99. Thiagarajan V, M. P, S. A, R. S, N. C, G.k. S, et al. Diminishing bioavailability and toxicity of P25 TiO2 NPs during continuous exposure to marine algae Chlorella sp. Chemosphere. 2019 Oct 1;233:363–72.

100. Dedman CJ, Rizk MMI, Christie-Oleza JA, Davies GL. Investigating the Impact of Cerium Oxide Nanoparticles Upon the Ecologically Significant Marine Cyanobacterium Prochlorococcus. Frontiers in Marine Science [Internet]. 2021 [cited 2023 Apr 10];8. Available from: https://www.frontiersin.org/articles/10.3389/fmars.2021.668097

101. Go EC, Pandey AS, MacRae TH. Effect of inorganic mercury on the emergence and hatching of the brine shrimpArtemia franciscana. Mar Biol. 1990 Feb 1;107(1):93–102.

102. Huang B, Wei ZB, Yang LY, Pan K, Miao AJ. Combined Toxicity of Silver Nanoparticles with Hematite or Plastic Nanoparticles toward Two Freshwater Algae. Environ Sci Technol. 2019 Apr 2;53(7):3871–9.

103. Yang H, Zhu Z, Xie Y, Zheng C, Zhou Z, Zhu T, et al. Comparison of the combined toxicity of polystyrene microplastics and different concentrations of cadmium in zebrafish. Aquatic Toxicology. 2022 Sep 1;250:106259.

104. Halldorsson S, Lucumi E, Gómez-Sjöberg R, Fleming RMT. Advantages and challenges of microfluidic cell culture in polydimethylsiloxane devices. Biosensors and Bioelectronics. 2015 Jan 15;63:218–31.

105. Lin L, Chung CK. PDMS Microfabrication and Design for Microfluidics and Sustainable Energy Application: Review. Micromachines (Basel). 2021 Oct 31;12(11):1350.

106. Hirama H, Otahara R, Kano S, Hayase M, Mekaru H. Characterization of Nanoparticle Adsorption on Polydimethylsiloxane-Based Microchannels. Sensors. 2021 Jan;21(6):1978.

107. Darmani H, Al-Saleh DRH. Lower Concentrations of the Glyphosate-Based Herbicide Roundup® Cause Developmental Defects in Artemia salina. Environ Toxicol Chem. 2023 Apr 21;

108. Quinlan GJ, Gutteridge JMC. Bacitracin and a Bacitracin-Zinc Complex Damage DNA and Carbohydrate in the Presence of Iron and Copper Salts. Free Radical Research Communications. 1989 Jan 1;7(1):37–44.

109. Trotman CNA, Mansfield BC, Tate WP. Inhibition of emergence, hatching, and protein biosynthesis in embryonic Artemia salina. Developmental Biology. 1980;80(1):167–74.

110. MacRae TH, Pandey AS. Effects of metals on early life stages of the brine shrimp, Artemia: a developmental toxicity assay. Arch Environ Contam Toxicol. 1991 Feb;20(2):247–52.

111. Foulkes EC. On the mechanism of transfer of heavy metals across cell membranes. Toxicology. 1988 Nov 30;52(3):263–72.

112. Braz-Mota S, Campos DF, MacCormack TJ, Duarte RM, Val AL, Almeida-Val VMF. Mechanisms of toxic action of copper and copper nanoparticles in two Amazon fish species: Dwarf cichlid (Apistogramma agassizii) and cardinal tetra (Paracheirodon axelrodi). Science of The Total Environment. 2018 Jul 15;630:1168–80.

113. Al-Bairuty GA, Shaw BJ, Handy RD, Henry TB. Histopathological effects of waterborne copper nanoparticles and copper sulphate on the organs of rainbow trout (Oncorhynchus mykiss). Aquatic toxicology. 2013;126:104–15.

114. Bilberg K, Malte H, Wang T, Baatrup E. Silver nanoparticles and silver nitrate cause respiratory stress in Eurasian perch (Perca fluviatilis). Aquatic Toxicology. 2010 Jan 31;96(2):159–65.

115. Saggese I, Sarà G, Dondero F. Silver Nanoparticles Affect Functional Bioenergetic Traits in the Invasive Red Sea Mussel *Brachidontes pharaonis*. BioMed Research International. 2016 Oct 5;2016:e1872351.

116. Black MN, Henry EF, Adams OA, Bennett JCF, MacCormack TJ. Environmentally relevant concentrations of amine-functionalized copper nanoparticles exhibit different mechanisms of bioactivity in Fundulus Heteroclitus in fresh and brackish water. Nanotoxicology. 2017 Sep 14;11(8):1070–85.

117. de Paiva Pinheiro SK, Lima AKM, Miguel TBAR, Pireda S, Fechine PBA, Souza Filho AG, et al. Acute toxicity of titanium dioxide microparticles in Artemia sp. nauplii instar I and II. Microscopy Research and Technique [Internet]. [cited 2023 Mar 30];n/a(n/a). Available from: https://onlinelibrary.wiley.com/doi/abs/10.1002/jemt.24312

118. Zhu S, Xue MY, Luo F, Chen WC, Zhu B, Wang GX. Developmental toxicity of Fe3O4 nanoparticles on cysts and three larval stages of Artemia salina. Environmental pollution. 2017;230:683–91.

119. Sorgeloos P, Remiche-Van Der Wielen C, Persoone G. The use of Artemia nauplii for toxicity tests—a critical analysis. Ecotoxicology and environmental safety. 1978;2(3–4):249–55.

120. Sorgeloos P, Dhert P, Candreva P. Use of the brine shrimp, Artemia spp., in marine fish larviculture. Aquaculture. 2001 Aug 15;200(1):147–59.

121. Støttrup J, McEvoy L. Live Feeds in Marine Aquaculture. John Wiley & Sons; 2008. 338 p.

122. Van Stappen G. 4.1. Introduction, biology and ecology of Artemia. Manual on the production and use of live food for aquaculture. 1996;

123. Vanhaecke P, Persoone G, Claus C, Sorgeloos P. Proposal for a short-term toxicity test with Artemia nauplii. Ecotoxicology and Environmental Safety. 1981 Sep;5(3):382–7.

124. Wang C, Jia H, Zhu L, Zhang H, Wang Y. Toxicity of α-Fe2O3 nanoparticles to Artemia salina cysts and three stages of larvae. Science of The Total Environment. 2017 Nov 15;598:847–55.

125. Pinheiro SK de P, Lima AKM, Miguel TBAR, Filho AGS, Ferreira OP, Pontes M da S, et al. Assessing toxicity mechanism of silver nanoparticles by using brine shrimp (Artemia salina) as model. Chemosphere. 2024 Jan 1;347:140673.

126. Kim L, Kim SA, Kim TH, Kim J, An YJ. Synthetic and natural microfibers induce gut damage in the brine shrimp Artemia franciscana. Aquatic Toxicology. 2021 Mar 1;232:105748.

127. Noventa S, Hacker C, Correia A, Drago C, Galloway T. Gold nanoparticles ingested by oyster larvae are internalized by cells through an alimentary endocytic pathway. Nanotoxicology. 2018 Sep 14;12(8):901–13.

128. Kummara S, Patil MB, Uriah T. Synthesis, characterization, biocompatible and anticancer activity of green and chemically synthesized silver nanoparticles – A comparative study. Biomedicine & Pharmacotherapy. 2016 Dec 1;84:10–21.

129. Ravichandran A, Subramanian P, Manoharan V, Muthu T, Periyannan R, Thangapandi M, et al. Phyto-mediated synthesis of silver nanoparticles using fucoidan isolated from Spatoglossum asperum and assessment of antibacterial activities. Journal of Photochemistry and Photobiology B: Biology. 2018 Aug 1;185:117–25.

130. Alaraby M, Abass D, Villacorta A, Hernández A, Marcos R. Antagonistic in vivo interaction of polystyrene nanoplastics and silver compounds. A study using Drosophila. Science of The Total Environment. 2022 Oct 10;842:156923.

131. Turna Demir F, Akkoyunlu G, Demir E. Interactions of Ingested Polystyrene Microplastics with Heavy Metals (Cadmium or Silver) as Environmental Pollutants: A Comprehensive In Vivo Study Using Drosophila melanogaster. Biology. 2022 Oct;11(10):1470.

132. Yang X, Gondikas AP, Marinakos SM, Auffan M, Liu J, Hsu-Kim H, et al. Mechanism of silver nanoparticle toxicity is dependent on dissolved silver and surface coating in Caenorhabditis elegans. Environmental science & technology. 2012;46(2):1119–27.

133. Mosleminejad N, Ghasemi Z, Johari SA. Ionic and nanoparticulate silver alleviate the toxicity of inorganic mercury in marine microalga Chaetoceros muelleri. Environ Sci Pollut Res [Internet]. 2024 Feb 15 [cited 2024 Mar 9]; Available from: https://doi.org/10.1007/s11356-024-32120-8

134. Greulich C, Braun D, Peetsch A, Diendorf J, Siebers B, Epple M, et al. The toxic effect of silver ions and silver nanoparticles towards bacteria and human cells occurs in the same concentration range. RSC Advances. 2012;2(17):6981–7.

135. Tallec K, Paul-Pont I, Boulais M, Le Goïc N, González-Fernández C, Le Grand F, et al. Nanopolystyrene beads affect motility and reproductive success of oyster spermatozoa (Crassostrea gigas). Nanotoxicology. 2020 Sep 13;14(8):1039–57.

136. Yang H, Xiong H, Mi K, Xue W, Wei W, Zhang Y. Toxicity comparison of nano-sized and micron-sized microplastics to Goldfish Carassius auratus Larvae. Journal of Hazardous Materials. 2020 Apr 15;388:122058.

137. Yaripour S, Huuskonen H, Rahman T, Kekäläinen J, Akkanen J, Magris M, et al. Pre-fertilization exposure of sperm to nano-sized plastic particles decreases offspring size and swimming performance in the European whitefish (Coregonus lavaretus). Environmental Pollution. 2021 Dec 15;291:118196.

138. Hu Q, Wang H, He C, Jin Y, Fu Z. Polystyrene nanoparticles trigger the activation of p38 MAPK and apoptosis via inducing oxidative stress in zebrafish and macrophage cells. Environmental Pollution. 2021 Jan 15;269:116075.

139. Wiklund AKE, Breitholtz M, Bengtsson BE, Adolfsson-Erici M. Sucralose – An ecotoxicological challenger? Chemosphere. 2012 Jan 1;86(1):50–5.

140. Zhu B, Wang Q, Shi X, Guo Y, Xu T, Zhou B. Effect of combined exposure to lead and decabromodiphenyl ether on neurodevelopment of zebrafish larvae. Chemosphere. 2016;144:1646–54.

141. Kashyap B, Frederickson LC, Stenkamp DL. Mechanisms for persistent microphthalmia following ethanol exposure during retinal neurogenesis in zebrafish embryos. Visual neuroscience. 2007;24(3):409–21.

142. Kalueff AV, Gebhardt M, Stewart AM, Cachat JM, Brimmer M, Chawla JS, et al. Towards a comprehensive catalog of zebrafish behavior 1.0 and beyond. Zebrafish. 2013;10(1):70–86.

143. Dong LL, Wang HX, Ding T, Li W, Zhang G. Effects of TiO2 nanoparticles on the life-table parameters, antioxidant indices, and swimming speed of the freshwater rotifer Brachionus calyciflorus. Journal of Experimental Zoology Part A: Ecological and Integrative Physiology. 2020;333(4):230–9.

144. Faimali M, Garaventa F, Piazza V, Greco G, Corrà C, Magillo F, et al. Swimming speed alteration of larvae of Balanus Amphitrite as a behavioural end-point for laboratory toxicological bioassays. Marine Biology. 2006 Apr 1;149(1):87–96.

145. Park J, Park CG, Sung B, Lee YO, Ryu CS, Park JY, et al. Acute Adverse Effects of Metallic Nanomaterials on Cardiac and Behavioral Changes in Daphnia Magna [Internet]. In Review; 2021 Feb [cited 2023 Jan 26]. Available from: https://www.researchsquare.com/article/rs-208731/v1

146. Pandey G, Madhuri S. Heavy metals causing toxicity in animals and fishes. Research Journal of Animal, Veterinary and Fishery Sciences. 2014;2(2):17–23.

147. Khayatzadeh J, Abbasi E. The Effects of Heavy Metals on Aquatic Animals. The 1st International Applied Geological Congress. 2010 Jan 1;26–8.